Study of low energy hadronic interaction models based on BESS observed cosmic ray proton and antiproton spectra at medium high altitude

Arunava Bhadra,[1,*] Sanjay K. Ghosh,[2,3,†] Partha S. Joarder,[3,‡] Arindam Mukherjee,[1,§] and Sibaji Raha[2,3,‖]

[1]*High Energy and Cosmic Ray Research Centre, University of North Bengal, Siliguri, West Bengal, India 734013*
[2]*Department of Physics, Bose Institute, 93/1 A.P.C. Road, Kolkata, India 700009*
[3]*Centre for Astroparticle Physics and Space Science, Bose Institute, Block EN, Sector V, Salt Lake, Kolkata, India 700091*

(Received 10 March 2009; published 23 June 2009)

We study low energy hadronic interaction models based on BESS observed cosmic ray proton and antiproton spectra at medium high altitude. Among the three popular low energy interaction models, we find that FLUKA reproduces the results of BESS observations on the secondary proton spectrum reasonably well over the whole observed energy range, the model UrQMD works well at relatively higher energies, whereas the spectrum obtained with GHEISHA differs significantly from the measured spectrum. The simulated antiproton spectrum with FLUKA, however, exhibits significant deviation from the BESS observation whereas UrQMD and GHEISHA reproduce the BESS observations within experimental error.

DOI: 10.1103/PhysRevD.79.114027 PACS numbers: 95.85.Ry

I. INTRODUCTION

Precise examination of the development of a cosmic ray shower in the earth's atmosphere is important in various contexts such as in the study of atmospheric neutrino oscillations or in the study of ultrahigh energy cosmic rays. The detailed process of development of such an extensive air shower (EAS) is, however, too complicated to be amenable to simple analytical descriptions. The main results concerning the flux and the other important features of the secondary cosmic ray particles in an EAS are thus obtained principally through the Monte Carlo (MC) simulation techniques.

MC simulations of the extensive air shower are strongly dependent on our knowledge of the interaction mechanisms of energetic particles. Such knowledge of particle interactions is somewhat uncertain at high energies as the accelerator data for relevant target-projectile combinations covering the whole kinematic region are not yet available. Even at very low (below $\sim$5 GeV) and low/intermediate (from few GeV to a few hundred GeV) energies, there is a lack of data on hadron-nucleus interactions and almost no measurements are available for the particle production in pion-nucleus collisions. One, therefore, relies mostly on theoretical models of particle interactions in such cases. The interaction models used in different simulation programs are necessarily extrapolations of known processes and/or of low energy accelerator data so that each model has its own parametrization guided by some (mainly QCD-motivated) theoretical prescriptions. The limited knowledge of particle interactions is considered to be one of the main sources of uncertainty in the estimation of the secondary particle flux in an EAS.

In view of the large uncertainties involved in the description of high energy particle interactions, the influence of high energy hadronic models on air shower observables has been a topic of active research for quite some time. Recent studies, however, suggest that the low energy hadronic interaction models also play a crucial role in the precise estimation of the low energy secondary cosmic ray flux in the atmosphere [1–3] simultaneously influencing some of the important characteristics of the extensive air showers. A strong dependence of the lateral particle distribution of the simulated extensive air showers at large core distances on the low energy hadronic interaction models has been reported [4].

The aim of the present work is to examine the sensitivity of the low to intermediate energy secondary proton and antiproton fluxes on the relevant hadronic interaction models. The simulated showers of secondary protons, which mainly arise from hadronic interactions of the forward kinematic region, are expected to be particularly responsive to the choice of interaction models. To generate secondary fluxes for various models of hadronic interactions, the air shower simulation program CORSIKA (cosmic ray simulation for Kascade) version 6.600 [5] is exploited here. A novel feature of the CORSIKA program is that it allows one to choose any of the three popular models, namely, GHEISHA [6], FLUKA [7], and UrQMD [8,9], for the portrayal of the low energy hadronic interactions as well as one of the seven different models, namely, DPMJET [10], HDPM [11], QGSJET 01 [12], SIBYLL [13–15], VENUS [16], NEXUS [17], and QGSJET II [18], for the description of hadronic interactions at high energies. The borderline between the high and the low energies is set as 80 GeV/n

*aru_bhadra@yahoo.com
†sanjay@bosemain.boseinst.ac.in
‡partha@bosemain.boseinst.ac.in
§aaarindam@yahoo.co.in
‖sibaji@bosemain.boseinst.ac.in

by default in this simulation program. Whether the low energy interaction models of CORSIKA can be discriminated *vis-à-vis* actual measurements will also be examined in this paper by comparing the simulated secondary proton and antiproton spectra obtained by using different low energy interaction models with the observations.

A practical problem in differentiating the influence of hadronic interaction models is that the estimation of secondary fluxes through MC simulations includes various systematic errors caused not only by the built-in uncertainties in the interaction models but also by the uncertainties involved in the estimation of values of various physical inputs, such as the primary cosmic ray fluxes, the atmospheric density profiles, etc. The effects of such errors on the calculation of physical inputs considerably complicate the simulated flux in such a way so as to make it difficult to isolate out the influence of interaction models alone on the calculated values of secondary fluxes. In particular, a dominant systematic error in evaluating the flux of cosmic ray secondaries arises from the uncertainties involved in the estimation of input fluxes of the primary cosmic rays. To minimize such uncertainties, the simulated results of secondary cosmic ray protons and antiprotons would be compared here with the recent precise measurements of such fluxes at the mountain altitude, at an atmospheric depth of 742 $\mathrm{g\,cm^{-2}}$, by the BESS spectrometer [19]. Also, the primary cosmic ray energy spectra, as measured by the same BESS instruments [20], would be considered in this paper as the inputs in the simulations after taking into account the effect of solar modulation that is appropriate for the specific period of the measurement of secondary fluxes by the BESS experiment.

The article is organized as follows: in the next section, we would provide a short account of the low/intermediate energy interaction models to be considered. The simulation procedure adapted in this work would be described in Sec. III. After a brief review of the precision measurements of hadronic and muon fluxes by the BESS spectrometer, the results of the simulations are compared with the corresponding observations in Sec. IV. Concluding remarks are given in Sec. V.

II. HADRONIC INTERACTION MODELS AT THE LOW TO INTERMEDIATE ENERGY RANGE

GHEISHA, UrQMD, and FLUKA are among the most popular hadronic interaction models in the low to intermediate energy range that would hereafter be referred as the ''low energy models'' in accordance with the terminology used in air shower simulations. These models find ample applications in various branches of physics and biophysics including the simulations of accelerator-based experiments, detector design, simulations of the cosmic rays, neutrino physics, radiotherapy, accelerator driven systems, etc. We have used FLUKA version 2006.3b, GHEISHA version 2002d, and UrQMD version 1.3 in the present work.

GHEISHA [6] is based on the parametrization of accelerator data. It was originally developed as an event generator in which the energy, momentum, charge, and the other quantum numbers are conserved only in the sense of an average instead of being conserved on an event-by-event basis. GHEISHA has been successfully used in the detector MC code GEANT [21] over the last 20 years and is currently being used as the default low energy interaction model in the EAS simulation program CORSIKA. A recent comparison with experimental data, however, exhibits a few shortcomings of the older version of GHEISHA [22,23]. The new version of the model (GHEISHA version 2002d), which has been used in the present work, incorporates certain modifications in kinematics through correction patches [23] thereby improving the energy and momentum conservation.

The simulation package FLUKA [7] describes particle interactions microscopically. It mainly employs resonance superposition models at the low energies (up to about 3–5 GeV), while relying on the two-string interaction model (the dual parton model) [24] at the intermediate energies. The basic conservation laws are obeyed at every single interaction level *a priori*. The resonance energies, widths, cross sections, and the branching ratios are extracted from the data and from the conservation laws by making explicit use of the spin and the isospin relations. In this model, the high energy hadron-nucleus interactions are described as a sequence of the Glauber-Gribov cascade, the generalized intranuclear cascade, preequilibrium emission and evaporation/fragmentation/fission and the final deexcitation, whereas, the nucleus-nucleus interactions above a few GeV/n are treated in FLUKA by interfacing with the DPMJET [10] model. A relativistic quantum molecular dynamics model [25] has been exploited at low energies to describe the nucleus-nucleus interactions.

In contrast, the UrQMD (ultrarelativistic quantum molecular dynamic) model [9] was originally designed for simulating relativistic heavy ion collisions in the energy range from around 1 AGeV to a few hundred AGeV that is the range of the (laboratory) energy in the case of the RHIC experiment. This microscopic model inherits the basic treatment of the baryonic equation of motion in the quantum molecular dynamic model and describes the phenomenology of hadronic interactions at low and intermediate energies in terms of the interactions between known hadrons and their resonances. The model does not use an intrinsic cross section calculation. Instead, the projectile is allowed to hit a sufficiently large disk involving maximum collision parameters as a result of which the program consumes rather long a CPU time. We may add here that both UrQMD and FLUKA describe fixed target data reasonably well.

III. ADAPTED SIMULATION PROCEDURE

The cosmic ray EAS simulation code CORSIKA [5] is widely used in various studies ranging from TeV gamma rays to the highest energy cosmic rays. Originally developed for the reproduction of extensive air showers with primary energies around the knee of the cosmic ray spectrum (i.e., around 10^{15} eV), CORSIKA has also found applications in the estimation of the flux of low energy secondary cosmic ray particles such as the neutrinos [1]. In the present work, the low energy hadronic interaction models FLUKA, GHEISHA, and the UrQMD have been used in combination with the high energy (above about 80 GeV/n) hadronic interaction model QGSJET 01 version 1c [12] in the framework of CORSIKA to generate secondary cosmic ray spectra. Because of the steeply falling energy spectrum of the primary cosmic rays, the contribution of the primary particles with energies above 80 GeV/n on the secondary proton spectrum is found to be only about 15% in our simulations. The high energy hadronic interaction models are, therefore, not likely to have much effect on the low energy secondary proton and antiproton spectrum.

The fluxes of secondary particles obtained by using CORSIKA have statistical as well as systematic errors. Apart from the uncertainties in the theoretical treatment of the hadronic interactions, the other major source of systematic error in the calculation of the secondary cosmic ray flux may, in fact, be the inaccuracies in the determination of absolute flux of the primary particles as was already mentioned in the Sec. I above. Some details on the primary spectrum and especially the effects of solar modulation and the geomagnetic field on such spectrum are, therefore, described in the following.

A. The primary spectra

In order to calculate the fluxes of the secondary cosmic rays, the primary cosmic ray energy spectrum is required as input in the simulations. The uncertainties in the determination of such primary flux have been substantially reduced in recent years with new precise measurements by the BESS (BESS-98 [20], the BESS-TeV [26]) and the alpha magnetic spectrometer [27,28] experiments. The detectors of such experiments were calibrated by using the accelerator beams thus ensuring the performance of those detectors. The spectra of primary cosmic ray protons observed by such experiments exhibit very good agreement with each other. Such an agreement is somewhat poorer in the case of the primary α particles, though being quite satisfactory for the purpose of our simulations. Also, the observed total primary nucleon flux below about 100 GeV, the dominant contribution to which is from the H nuclei, is found to agree within an accuracy of 4.0% in the above three experiments [3,29]. For such reasons, we arbitrarily choose the BESS-98 primary spectra as the input primary spectra in our EAS simulations as described in the following.

The BESS mission collected data for the absolute fluxes of primary protons and helium nuclei down to 1.0 GeV [20]. The effect of the so-called *solar modulation*, however, introduces a prominent time dependence on the absolute flux of the primary particles below about 10 GeV. The effect of such solar modulation may be handled by using a simple *force field approximation* [30,31], according to which the differential intensity $J_i(T, \psi(t))$ of cosmic ray nuclei of the species i with a charge number Z and a mass number A that have a kinetic energy T (in MeV per nucleon) at a distance of 1 AU from the sun is given by [32]

$$J_i(T, \psi(t)) = J_{\mathrm{LIS},i}(T + \psi(t)) \times \frac{T(T + 2m_o)}{(T + \psi(t))(T + \psi(t) + 2m_o)}, \quad (1)$$

where $m_o = 938$ MeV is the proton rest mass and $\psi(t) = (Ze/A)\phi(t)$ with $\phi(t)$ being a *solar modulation potential* in MV. Here, $J_{\mathrm{LIS},i}$ denotes the local interstellar spectrum of the cosmic ray nuclei of type i at (practically) infinite distance from the Sun. Depending on the solar activity, the modulation potential $\phi(t)$ may be obtained by using theoretical models. Accordingly, for each period of the solar cycle, the incident cosmic ray flux may be corrected for different solar modulation effects using the above equation.

In the following, we incorporate the force field approximation in the CORSIKA program and consider an energy dependence for interstellar cosmic ray intensity as prescribed by [33]. Such a dependence is given by

$$J_{\mathrm{LIS}}[T] = \frac{J_o P(T)^{-2.78}}{1 + 0.4866 P(T)^{-2.51}}, \quad (2)$$

where J_o is a normalization factor and $P(T) = \sqrt{T(T + 2m_o)}$. By using CORSIKA, we next generate the primary energy spectra (without considering the geomagnetic cutoff) for the primary protons and the α particles by considering $\phi = 0.565$ GeV as the value of the solar modulation potential that is applicable to the BESS 98 flight [32]. Such primary spectra are then compared with the BESS observation of the primary proton and the He spectra [20], as shown in the Figs. 1 and 2, respectively.

It is clear from the figures that the agreement between the simulated spectra and the observations is quite satisfactory. Subsequently, for the BESS high altitude measurement of the secondary proton and the antiproton fluxes in September 1999, the primary cosmic ray spectra are generated taking a solar modulation potential $\phi = 0.685$ GeV [32] into account. It is to be noted that, in obtaining the above spectra for the primary protons and the α particles, we allowed the energy of such particles to vary between the minimum of the geomagnetic cutoffs (see the explanation below) and a maximum energy of 10^{14} eV.

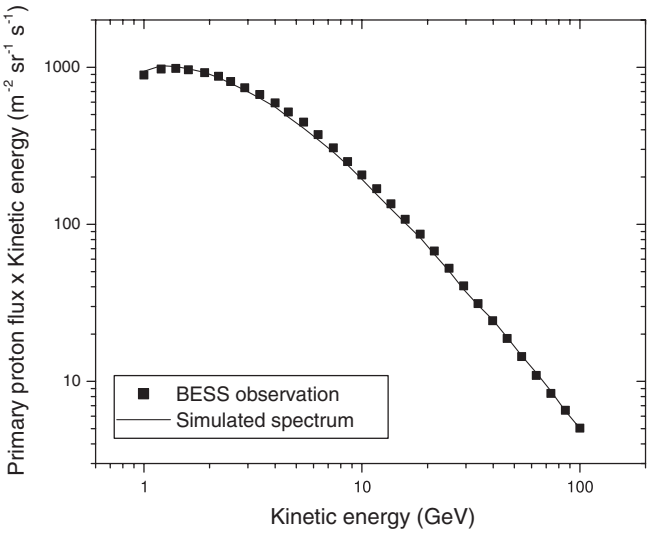

FIG. 1. Comparison of simulated primary proton spectrum with the BESS 1998 observation.

B. The geomagnetic cutoff

The Earth's magnetic field imposes a cutoff energy below which the primary cosmic rays cannot penetrate the atmosphere. Such geomagnetic cutoff is an important ingredient of simulation for the estimation of the secondary particle fluxes in an EAS as it affects the primary cosmic ray flux at a particular location on the Earth. It also produces the zenith and the azimuth angle variation of cosmic ray flux at each position. We may here note that, for the measurement of the primary cosmic ray spectra [20], the BESS spectrometer was flown from Lynn Lake, Canada where the vertical geomagnetic rigidity cutoff is quite small, being only about 0.5 GV. For this reason, the geomagnetic cutoff has not been taken into account for reproducing the BESS 1998 data in Figs. 1 and 2. However, the BESS experiment measured the secondary proton spectrum at Mt. Norikura, Japan, where the vertical rigidity cutoff is much larger, being around 11.2 GV in magnitude. A precise estimation of the geomagnetic cutoff is, therefore, important for reproducing the secondary proton spectrum at Mt. Norikura.

The geomagnetic rigidity cutoff needs to be computed for each primary cosmic ray particle. In the present work, the geomagnetic cutoff calculations have been performed using the (back) trajectory-tracing technique [34]. The quiescent international geomagnetic reference field model for 1995 [35] of the Earth's magnetic field has been used for such cutoff calculations. In reality, the cosmic ray rigidity cutoff may not take a unique value; a penumbra region may exist in the particle rigidity range for a particular direction. In the penumbra region, a complex series of allowed and forbidden cosmic ray trajectories coexists and an effective rigidity cutoff is obtained considering the transmission through the penumbra. The mean geomagnetic rigidity cutoff obtained from the calculations for cosmic ray particles entering the atmosphere at the location of Mt. Norikura from different directions are shown in Fig. 3.

The penumbra region of the cutoff at the Mt. Norikura location is shown in Fig. 4. The width of the penumbra region at the Mt. Norikura location is found to vary from 0.0 GV to about 4.0 GV in some particular directions.

The geomagnetic rigidity cutoff calculations have been used to modify the primary cosmic ray spectra obtained from the CORSIKA. The bending of the charged particles in the Earth's magnetic field during the development of the

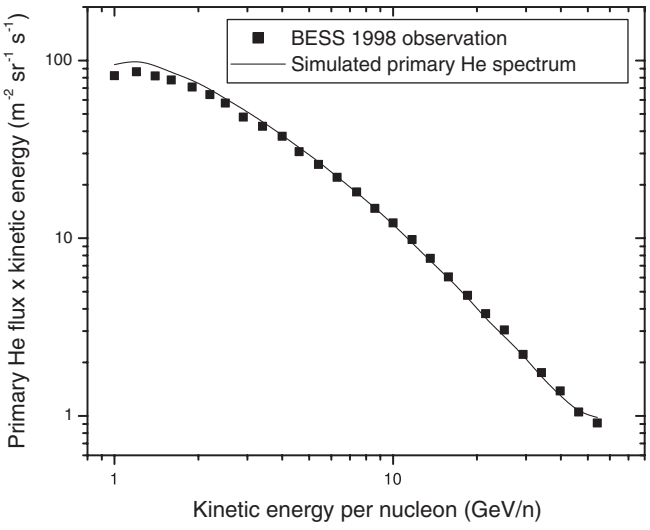

FIG. 2. Comparison of simulated primary α particle spectrum with the BESS 1998 observation.

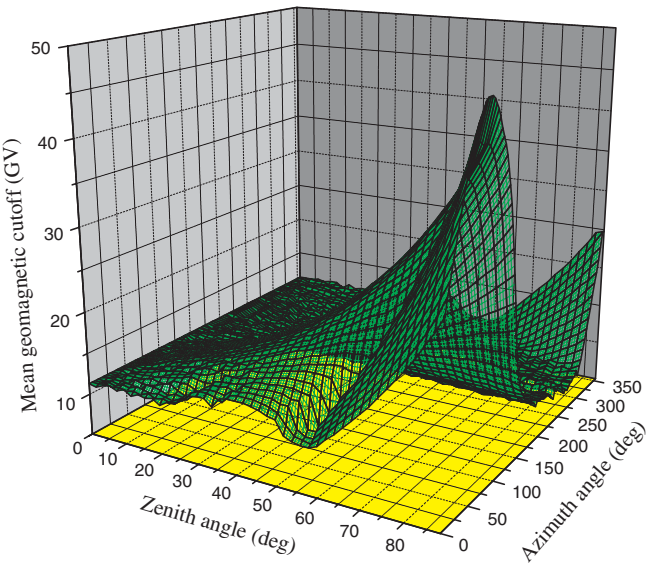

FIG. 3 (color online). Directional dependence of the mean geomagnetic cutoff for primary cosmic rays at the location of Mt. Norikura.

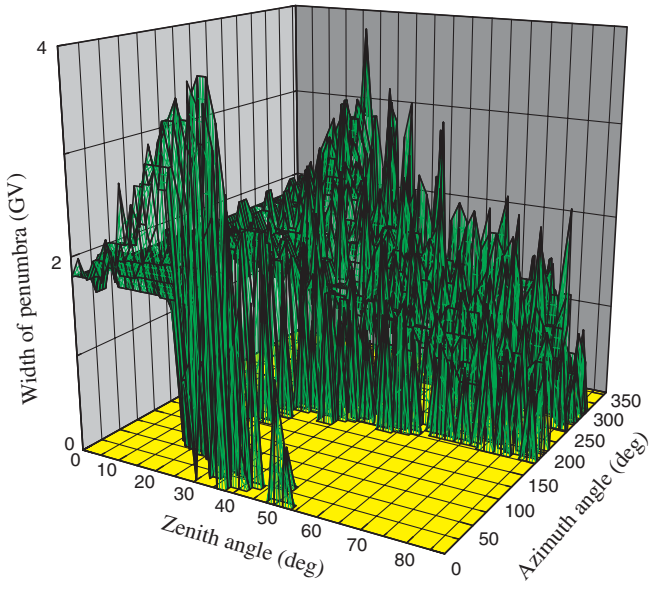

FIG. 4 (color online). The width of the geomagnetic penumbra region at the location of Mt. Norikura.

EAS is, however, taken into account by the CORSIKA program itself.

C. Other settings

The fluxes of the cosmic ray secondaries also depend on the atmospheric density profile. We consider the U.S.-standard atmospheric model [36] with a planar approximation in the present work. Such a model of the atmosphere has been found to be reasonable for describing the atmospheric muon spectra at high altitude [2]. The planar approximation works only in the case of the zenith angle for the primary particles being less than 70°. As the BESS observation of the secondary cosmic rays was restricted to zenith angles much smaller than 70° (see below), the planar approximation seems to be sufficient to simulate such an observational situation. Moreover, the validity of such approximation for the primary zenith angle has also been checked in the present analysis by first generating data with the "CURVED" version of CORSIKA [37]. We considered a particular set of input parameters with a primary zenith angle chosen to be in the range of 0° to 89° in this particular simulation. The results of such a simulation are then compared with those given by the planar version of the CORSIKA program with an identical set of input parameters but with a maximum primary zenith angle now being less than 70°. The primary and the secondary spectra obtained from the two programs agree with each other to high accuracy. Further details of such a comparison are, however, excluded in this paper for the sake of brevity.

Proton, helium, and the heavier nuclei up to iron are considered here as the primary particles of an EAS. However, instead of taking each of the elements individually, the primary nuclei heavier than helium are taken in three separate groups, namely, the medium ($5 < Z < 10$, $\langle A \rangle \approx 14$), heavy ($11 < Z < 20$, $\langle A \rangle \approx 24$), and the very heavy ($21 < Z < 30$, $\langle A \rangle \approx 56$) nuclei, respectively. The spectra for those groups are taken from the compilation of [38]. The sum of the fluxes of individual elements is taken as the flux of a group, and for power index the weighted average value is used. Contributions of each variety of the primary particles to the secondary proton/antiproton fluxes have been separately estimated. Such individual contributions are finally summed up to get the resultant secondary flux of protons and antiprotons in the EAS. Nearly (2–7) $\times$ 10^7 events have been generated here for the estimation of the fluxes of such secondary particles.

IV. SIMULATED RESULTS AND COMPARISON WITH OBSERVATION

Only a few measurements of the cosmic ray proton fluxes at the mountain altitude have been reported so far. The most recent of such observations is due to the BESS group [19] that used a high resolution spectrometer with a large acceptance area consisting of a superconducting magnet and a drift chamber based tracking system. Both the atmospheric proton and antiproton spectra at Mt. Norikura at an atmospheric depth of 742 g cm^{-2} were measured in this observation. A threshold-type aerogel Cherenkov counter was used there to distinguish protons and antiprotons from the muons. Besides, the experiment was equipped with an electromagnetic shower counter to separate electrons and positrons from the muons for the muon analysis. The range of kinetic energy covered in the above experiment was 0.25 to 3.3 GeV/c.

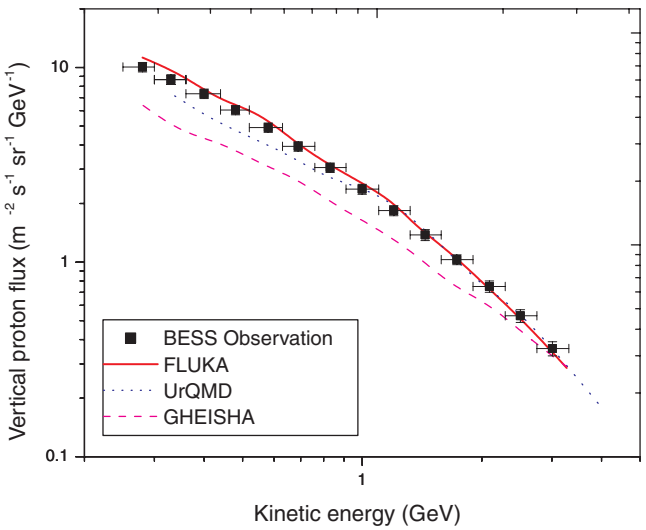

FIG. 5 (color online). The differential spectra of vertical proton at Mt. Norikura obtained by using three low energy models as is described in the text. The results of the BESS observation is also given for comparison.

In Fig. 5, the vertical proton spectra, as obtained from the CORSIKA simulations by using all three low energy interaction models at the location of Mt. Norikura, are plotted and compared with the observation of the BESS experiment. In the observation, the zenith angle (θ_z) of the measurements was limited to $\cos\theta_z \geq 0.95$. The same restriction on the zenith angle has been retained here in deriving the simulated proton spectra in Fig. 5. The (statistical) errors in simulated spectra are quite small, and fall within the thickness of the representing lines.

It is clear from Fig. 5 that only the FLUKA model satisfactorily describes the observed data over the whole energy range. The GHEISHA and the UrQMD give lower proton flux at the low energy end than the BESS results. In the case of GHEISHA, in particular, the simulated results are found to be substantially lower than the BESS observations over the entire range. The spectrum obtained by using the UrQMD and the QGSJET combination shows reasonable agreement with the observations above a secondary proton energy of 1 GeV but differs at lower energies. To ensure that the discrepancy at the low energy end originates from UrQMD but not from QGSJET, the secondary proton spectrum was also generated (not shown in this paper) by using the UrQMD and the NEXUS combination that showed an almost identical deviation from the observations at the low energy end. Results obtained from all the three low energy models are, however, found to approach each other at the higher energy range.

The comparison of the calculated zenith angle dependence of proton flux for two different kinetic energy ranges (0.30–0.36 and 1.90–2.29 GeV, respectively) with the ones observed by the BESS experiment [19] at Mt. Norikura is shown in Fig. 6. While calculating the fluxes in this figure, we select only those events in our MC simulations that satisfy $\cos\theta_z \geq 0.85$ to be consistent with the BESS observation. Although the simulated results contain some fluctuations that are of statistical origin, it seems to be evident from the plot that the nature of variation of the simulated proton flux with the zenith angles is in accordance with the BESS observation for all three low energy interaction models under consideration. However, the proton fluxes obtained by using GHEISHA is found to be somewhat lower than that found in the observation over the whole range of zenith angles, particularly at the lower energy bin.

The cosmic ray induced $\bar{p}$ flux in the atmosphere has been measured at the mountain level by the BESS experiment and is expected to be purely of an atmospheric origin [19]. The simulated results for the antiproton spectra are compared with observations in Fig. 7. Surprisingly, the FLUKA program could not reproduce the observed antiproton data well, whereas the antiproton spectrum due to UrQMD is found to be consistent with the observational results within the experimental error. GHEISHA too represents the observed data well. The production spectrum of

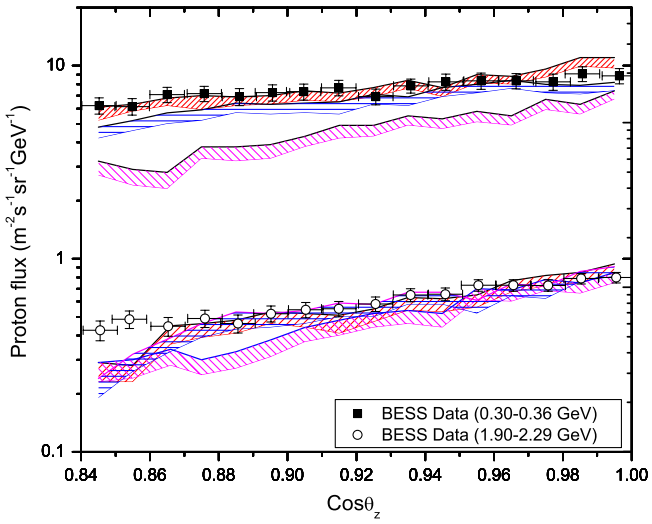

FIG. 6 (color online). The zenith angle dependence of the proton flux at the location of Mt. Norikura for two different kinetic energy bins obtained for three low energy models in comparison with the BESS observation. The band shaded by the left-tilted lines corresponds to simulated spectrum due to the FLUKA model. Similarly, the band shaded by almost horizontal lines corresponds to the UrQMD model, and the band shaded by the right-tilted lines corresponds to the GHEISHA model.

$\bar{p}$ is known to peak around 2 GeV [39]. Because of the propagation in the atmosphere, this spectral peak shifts towards lower energies as is clearly revealed from Fig. 7.

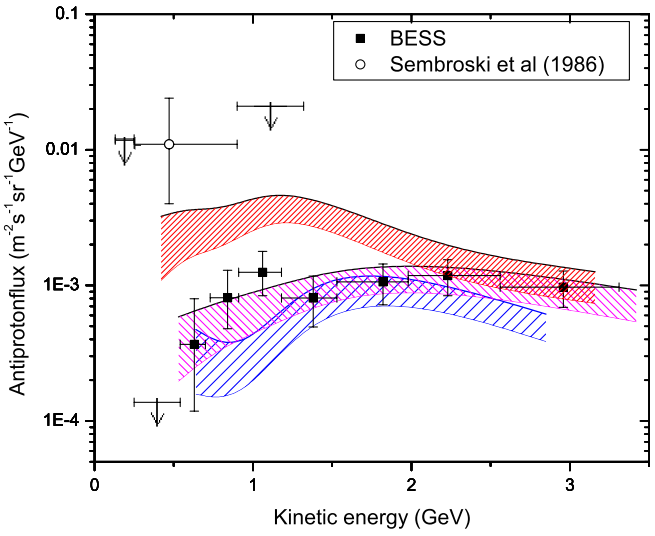

FIG. 7 (color online). The differential spectra of vertical antiproton at Mt. Norikura obtained for three low energy models. The band shaded densely by the left-tilted lines corresponds to the simulated spectrum due to the FLUKA model. Similarly, the band shaded lightly by the left-tilted lines corresponds to the UrQMD model, and the band shaded by the right-tilted lines corresponds to the GHEISHA model. The results of the BESS observation and those obtained by [43] in a similar observational condition are also given for comparison.

V. CONCLUSION

From the results of our CORSIKA simulations that are presented in the previous section, we may arrive at the following conclusions.

(1) The fluxes of cosmic ray secondary protons and antiprotons at mountain altitude are found to be quite sensitive to the low energy interaction models. The secondary protons arise mainly from hadronic interactions in the forward kinematic region (they mainly come from valence quark recombination, only a small fraction of the observed protons could have been produced centrally), whereas muons come from the central region of the interactions. Consequently, secondary protons of the same energy as the muons are produced from primaries of comparatively lower energies. For instance, muons with kinetic energy of 2 GeV or more are produced predominantly by 40 to 100 GeV primary particles, whereas a significant fraction of protons of similar energy are produced by primary particles of energies less than 40 GeV. Hence, the secondary protons not only probe the models in the forward kinematic range but they are more responsive to the low energy models than the muons or the neutrinos [40] in the concerned energy region.

(2) The present analysis suggests that, among the three low energy models admissible in CORSIKA, only the FLUKA model produces a secondary proton spectrum in consistence with the BESS observation over the whole observed energy range. The model UrQMD works well at relatively higher energies, whereas the spectrum obtained with GHEISHA exhibits significant deviation from the measured spectrum; i.e., it generates too few protons in general.

In a recent study, [2] compared simulation results of the atmospheric muon flux by using the low energy interaction models FLUKA and UrQMD with the observations. They noticed that the simulated muon fluxes for the two models differ considerably from each other at lower energies though the results for both the models are consistent with the observed results within experimental error. The BESS observation of the proton spectrum at mountain level, however, clearly favors FLUKA over the UrQMD model at relatively lower energies. Note that, like the proton flux, the muon flux obtained with UrQMD has also been found to be lower than that obtained with FLUKA at lower energies [2]. Besides, the muon charge ratio $[N(\mu^+)/N(\mu^-)]$ obtained with UrQMD was also found to be lower than the experimental results, especially for low and intermediate energies [1]. The predictions of GHEISHA, both on the muon flux and on the muon charge ratio, differ considerably from observation [1].

The inability of GHEISHA to reproduce the BESS observation is not totally unexpected as it has been revealed from recent studies that the model could not properly replicate the pion and kaon production spectra in hadron-nucleus interactions observed in accelerator experiments [4,23]; the model does not satisfy many of the conservation laws in a single hadronic interaction. It is worth mentioning here that, for generation of secondary cosmic rays, hadron-nucleus collisions are more relevant, with nitrogen being the most important target nucleus and the inclusive cross section for production of a secondary particle in hadron-nucleus interactions is the most important factor in atmospheric flux estimation for the secondary particle. Though the recent version of GHEISHA incorporates certain modifications in kinematics to overcome the issue of violation of conservation laws, the present study shows that the model still has serious limitations in describing the atmospheric proton spectrum. Since GHEISHA is an empirical model, it is not unlikely that the model will exhibit shortcomings in the regions where experimental data are not available.

In the UrQMD model particle production takes place either via the decay of a meson or baryon resonance or via string excitation and fragmentation. The leading hadrons of the fragmenting strings contain the valence quarks of the original excited hadron. The UrQMD model (as well as other microscopic models) calculates the inclusive cross sections for production of various secondary particles in hadron-nucleus interactions from the properties of hadron-hadron interactions which are fed into the model as basic inputs. In this model, the hadronic cross sections are treated as a function of the incoming and outgoing particle types, their isospins and their center-of-mass energy. An effective parametrization of various cross sections is employed in the UrQMD model based on simple phase space considerations; free parameters are tuned to experimental measurements (in the absence of quality experimental data, they are extracted from other cross sections via general principles with approximations). The prediction of the model on the multiplicities of prominent secondary particles produced in proton-proton collisions at laboratory energy about 12 GeV lies within 15% (10% for proton) of the accelerator data and at an energy of about 200 GeV it falls within 10% (2% for proton) of the experimental data [9]. The UrQMD is slightly lower in multiplicity than the FLUKA [4]. For hadron-nucleus interactions the predictions of the model on production spectra of pions, kaons, etc. have been tested with experimental data [23] but adequate comparison of the model predictions on leading particle distribution with observational data could not be made due to a lack of quality experimental measurements. The mountain altitude measurements of secondary cosmic ray proton spectra, like the one by BESS, offer an indirect opportunity in this regard. It seems that the overall performance of the model in respect to atmospheric secondary flux estimation at low energies may improve with an appropriate choice of the free parameters of the model. It is also important to confirm whether the discrepancies are due to some additional nuclear effects, which are not included in the UrQMD model.

The FLUKA describes the BESS observation on the secondary low energy cosmic ray proton spectrum reasonably well. Being based on theoretical microscopic models, it has the advantage over the parametrized inclusive models, of preserving correlations. The model parameters are fixed once (initially) for all projectile-target combinations and energies. In recent times the model has shown its strength in reproducing experimental data (on pion production spectrum in proton-carbon interactions) recently obtained by the HARP [41] and NA49 Collaborations [42]. The present comparison indicates the success of the model in describing leading particle distribution.

(3) The simulated $\bar{p}$ spectrum with the FLUKA model shows significant disagreement with the BESS observation. Fluxes obtained with FLUKA are found to be significantly higher than the observed fluxes though the difference between the simulated and the observed fluxes decrease at higher energies. The antiproton flux generated in this paper by using FLUKA is, however, found to be lower than those obtained by the High Energy Physics group of the University of Arizona [43] in an experiment under similar observational conditions (i.e., at a comparable atmospheric depth of about 747 $\mathrm{g\,cm^{-2}}$). Similar discrepancies between the simulated flux and that obtained from the BESS observations at low energies have also been noticed in [39,44,45], while the simulations in [46,47] are found to reproduce the BESS data satisfactorily. All such calculations used empirical expressions of $\bar{p}$ production and annihilation cross sections that are based on the parametrization of measured data. It was earlier reported that the UrQMD 1.3 predictions on multiplicity of $\bar{p}$ in the inelastic pp interactions overestimate the experimental data [48] in the super proton synchrotron domain. Here, the energy range is somewhat lower but the agreement of the model prediction with observation is quite well.

For the given cosmic ray fluxes at the top of the atmosphere, the $\bar{p}$ flux at mountain altitude mainly relies on two factors: the inclusive $\bar{p}$ production cross section in the cosmic ray-air nuclei collisions and the propagation of $\bar{p}$ inside the atmosphere. The latter factor includes ionization energy loss, loss of $\bar{p}$ due to annihilation, and other interactions. The noted discrepancy of FLUKA-derived results with the observations thus could be either due to enhanced production of $\bar{p}$ or due to the suppression of $\bar{p}$ annihilation or even due to both of these effects. From a preliminary analysis, we note that even at very high altitude, the $\bar{p}$ flux due to FLUKA remains higher than that due to UrQMD or GHEISHA, which primarily indicates that the antiproton production is enhanced in FLUKA at low energies. The basic $\bar{p}$ production reaction is the inclusive $NN \rightarrow \bar{p}X$ process with N standing for the nucleon and X for any final hadronic state allowed in the process. The cross section data for the proton induced inclusive $\bar{p}$ production on nuclei and on the nucleons are not very accurate, particularly at energies around and below 1 GeV because of the lack of accelerator data over such an energy range. Besides, no reliable estimate of the low energy $\bar{p}$ production in cosmic ray- atmospheric nucleus collision can be made presently due to the high sensitivity to nuclear medium effects. The BESS results offer an indirect way to examine the $\bar{p}$ production at low energies. However, in view of the large discrepancies between the observational results obtained by the BESS and the University of Arizona group, more experimental results seem to be necessary to arrive at definite conclusions regarding the correctness of a $\bar{p}$ production mechanism in the FLUKA model.

ACKNOWLEDGMENTS

We thank an anonymous referee for useful comments and suggestions. S. K. G., P. S. J., and S. R. thank the Department of Science and Technology (Government of India) for support under the IRHPA scheme.

[1] J. Wentz *et al.*, Phys. Rev. D **67**, 073020 (2003).
[2] T. Djemil, R. Attallah, and J. N. Capdevielle, J. Phys. G **34**, 2119 (2007).
[3] T. Sanuki *et al.*, Phys. Rev. D **75**, 043005 (2007).
[4] H. J. Drescher *et al.*, Astropart. Phys. **21**, 87 (2004).
[5] D. Heck *et al.*, Forschungszentrum Karlsruhe Report No. FZKA 6019, 1998.
[6] H. Fesefeldt, RWTH Aachen Report No. PITHA-85/02, 1985.
[7] A. Fassò *et al.*, in *Proceedings of the Monte Carlo 2000 Conference (Lisbon)* (Springer, Berlin, 2001), p. 955.
[8] S. A. Bass *et al.*, Prog. Part. Nucl. Phys. **41**, 225 (1998).
[9] M. Bleicher *et al.*, J. Phys. G **25**, 1859 (1999).
[10] J. Ranft, Phys. Rev. D **51**, 64 (1995).
[11] J. N. Capdevielle *et al.*, Kernforschugszentrum Karlsruhe Report No. KfK 4998, 1992.
[12] N. N. Kalmykov, S. S. Ostapchenko, and A. I. Pavlov, Nucl. Phys. B, Proc. Suppl. **52**, 17 (1997).
[13] R. Engel *et al.*, Phys. Rev. D **46**, 5192 (1992).
[14] R. Engel *et al.*, in Proceedings of the 26th International Cosmic Ray Conference, Salt Lake City, USA, 1999, Vol. 1, p. 415.
[15] R. S. Fletcher *et al.*, Phys. Rev. D **50**, 5710 (1994).
[16] K. Werner, Phys. Rep. **232**, 87 (1993).
[17] H. J. Drescher *et al.*, Phys. Rep. **350**, 93 (2001).
[18] S. S. Ostapchenko, Nucl. Phys. B, Proc. Suppl. **151**, 143 (2006).
[19] T. Sanuki *et al.*, Phys. Lett. B **577**, 10 (2003).

[20] T. Sanuki *et al.*, Astrophys. J. **545**, 1135 (2000).
[21] "GEANT: Detector Description and Simulation Tool," CERN Program Library W5013 (CERN, Geneva).
[22] A. Ferrari and P. R. Sala, CERN, Geneva ATLAS internal note PHYS-No-086, 1996.
[23] D. Heck, Nucl. Phys. B, Proc. Suppl. **151**, 127 (2006).
[24] A. Capella *et al.*, Phys. Rep. **236**, 225 (1994).
[25] H. Sorge, Phys. Rev. C **52**, 3291 (1995).
[26] S. Haino *et al.*, Phys. Lett. B **594**, 35 (2004).
[27] J. Alcaraz *et al.*, Phys. Lett. B **472**, 215 (2000).
[28] J. Alcaraz *et al.*, Phys. Lett. B **494**, 193 (2000).
[29] T. K. Gaisser *et al.*, in Proceedings of the 27th International Cosmic Ray Conference, Hamburg, Germany, 2001, Vol. 5, p. 1643.
[30] L. G. Gleeson and W. I. Axford, Astrophys. J. **154**, 1011 (1968).
[31] K. G. McCracken *et al.*, J. Geophys. Res. **109**, A12103 (2004).
[32] I. G. Usoskin *et al.*, J. Geophys. Res. **110**, A12108 (2005).
[33] R. A. Burger, M. S. Potgieter, and B. Heber, J. Geophys. Res. **105**, 447 (2000).
[34] M. A. Shea and D. F. Smart, J. Geophys. Res. **72**, 2021 (1967).
[35] T. J. Sabaka *et al.*, J. Geomag. Geoelectr. **49**, 157 (1997).
[36] J. Linsley (private communication).
[37] D. Heck, Forschungszentrum Karlsruhe Report No. FZKA 6954, 2004.
[38] B. Weibel-Sooth, P. L. Biermann, and H. Mayer, Astron. Astrophys. **330**, 389 (1998).
[39] S. A. Stephens, Astropart. Phys. **6**, 229 (1997).
[40] G. Battistoni *et al.*, Astropart. Phys. **17**, 477 (2002).
[41] M. G. Catanesi *et al.*, Nucl. Phys. **B732**, 1 (2006).
[42] C. Alt *et al.*, Eur. Phys. J. C **49**, 897 (2007).
[43] G. H. Sembroski *et al.*, Phys. Rev. D **33**, 639 (1986).
[44] T. Bowen and A. Moats, Phys. Rev. D **33**, 651 (1986).
[45] S. A. Stephens, Adv. Space Res. **35**, 142 (2005).
[46] C. Y. Huang, L. Derome, and M. Buenerd, Phys. Rev. D **68**, 053008 (2003).
[47] R. Duperray *et al.*, Phys. Rev. D **71**, 083013 (2005).
[48] M. Bleicher *et al.*, Phys. Lett. B **485**, 133 (2000).